

# Transport analysis of the thermalization and energy relaxation of photoexcited hot electrons in Ge-doped GaAs

P. Supancic

*Institut für Struktur- und Funktionskeramik, Montanuniversität, A-8700 Leoben, Austria*

U. Hohenester and P. Kocevar

*Institut für Theoretische Physik, Karl-Franzens-Universität, A-8010 Graz, Austria*

D. Snoke,\* R. M. Hannak, and W. W. Rühle

*Max-Planck Institut für Festkörperforschung, D-70506 Stuttgart, Germany*

(Received 9 June 1995; revised manuscript received 6 November 1995)

A very fast broadening, thermalization, and cooling of an initially narrow photoexcited electron distribution was recently observed in the time- and frequency-resolved electron-acceptor luminescence of *p*-type bulk GaAs:Ge for near-band-gap excitation at low excitation densities and temperatures. As the short thermalization times could not be explained by the standard rates for the conventional carrier-carrier, carrier-impurity, and carrier-phonon scatterings, unconventional types of thermalizing carrier interactions were originally suggested to interpret the data. In contrast, the present analysis restricts itself to the conventional scattering mechanisms, but attempts to explain the fast thermalization and cooling rates by accounting for the finite experimental pulse-repetition rates and the resulting presence of neutral donors of the amphoteric germanium, causing a very effective additional electronic energy-relaxation channel via impact ionizations of Ge donors.

## I. INTRODUCTION AND EXPERIMENTAL BACKGROUND

Time- and frequency-resolved hot-carrier luminescence has for many years provided an important tool for the study of relaxation processes in highly laser-pulse-excited electron-hole (*e-h*) plasmas in semiconductors. Ultrafast excitation and luminescence-upconversion techniques have been used to follow the downrelaxation of carriers from their photo-populated band regions toward their respective band minima with a time resolution of less than 100 fs.<sup>1-3</sup> Luminescence spectroscopy with lower time resolution and correspondingly higher frequency resolution has allowed the study of finer details of the state occupations and band structures.<sup>4-6</sup>

Ordinary interband luminescence across the band gap yields the product of the electron and hole distribution functions for each of the optically coupled band regions, and in general the individual distribution functions can only be obtained in combination with a detailed theoretical analysis of the experimental data.<sup>2,3</sup> In contrast, electron-acceptor luminescence has the advantage of involving only one type of free carriers. For the present case of time-resolved luminescence spectroscopy of a direct-gap material, this allows us to monitor directly the distribution function and thereby the scattering dynamics of the photoexcited electrons as functions of time.<sup>7-9</sup>

Here, near-band-gap excitation, with electronic excitation energies below the threshold for optical-phonon emission, and low lattice temperatures have the further advantage of eliminating noticeable phononic contributions to the initial relaxation of the photogenerated carriers. In this way one can hope to study the purely Coulombic scattering dynamics within the coupled system of electrons, holes, and impurities, and in particular the broadening and eventual thermalization

of the initially narrow photoexcited electron distribution.

In spite of some recent progress in the theoretical description of nonequilibrium Coulomb systems,<sup>3,10-14</sup> it came as a surprise when a very fast broadening, thermalization, and cooling of photoexcited electron distributions during and after near-band-gap excitation was detected in moderately Ge-doped *p*-GaAs ( $p = 5 \cdot 10^{16} \text{ cm}^{-3}$ ) at *extremely low* photoexcitation densities ( $4 \times 10^{14}$  and  $4 \times 10^{13}$  pairs per  $\text{cm}^3$ ).<sup>8,9</sup> The *e-h* band-to-band excitation was achieved by 5-ps laser pulses with a photon energy of 1.536 eV (17-meV excess energy per *e-h* pair), and the luminescence detected with a streak camera of 15-ps time resolution and a spectral resolution of 1 meV. The experimental thermalization times were obtained from the temporal evolution of the measured spectra toward a purely exponential frequency dependence, reflecting the approach to a thermalized, i.e., Maxwellian, electron distribution.

The lattice temperatures (10 K) were low enough to ensure a significant electron-acceptor luminescence, and to eliminate decisive phononic effects. Nevertheless, the theoretical estimates in terms of the conventional transition rates for the carrier-carrier scatterings yielded thermalization times much longer than those extracted from the experimental spectra.<sup>8,9</sup>

To estimate a possible role of spatial inhomogeneities, measurements were performed on both bulk and appropriately structured samples, the latter to limit vertical diffusion and surface recombination processes. It turned out that the luminescence data were the same for both types of samples. This excluded the possibility that the bulk data contained dominant luminescence contributions from regions with electron densities higher than the average nominal densities and with a correspondingly higher electronic thermalization rate.

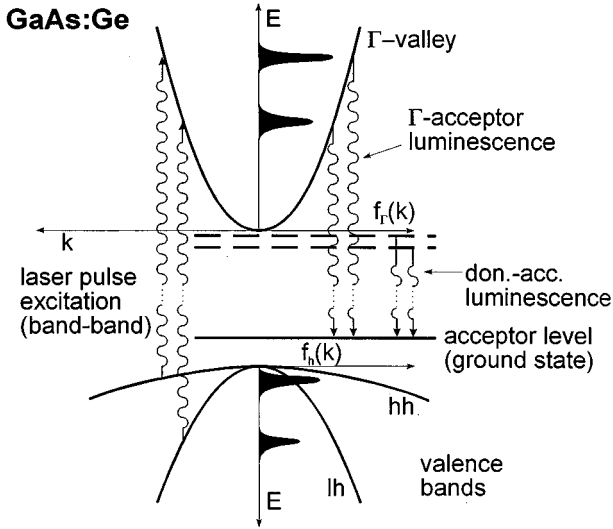


FIG. 1. Schematic picture of the band-acceptor luminescence spectroscopy in GaAs:Ge.

Figure 1 gives a schematic picture of the band-acceptor luminescence spectroscopy of Ge-doped GaAs, including the excitation channel from both the heavy-hole (hh) and light-hole (lh) valence bands, and indicating the participation of Ge-donor levels. The full lines in Fig. 2 present the measured band-to-acceptor luminescence for the two excitation densities of  $4 \times 10^{14}$  and  $4 \times 10^{13} \text{ cm}^{-3}$  on a linear scale at four different times, with the time zero taken at the center of the excitation pulse. In Fig. 3 these data were divided by the density of states in order to depict directly the distribution function of the electrons on a semilogarithmic plot. As a Maxwellian distribution should give a straight line, this type of presentation very clearly reveals deviations from internally thermalized distributions.

In view of the very low excitation densities, the most striking feature of the experimental data is the strong broadening of the spectra with respect to the narrow excitation spectrum (dotted lines in Fig. 2) already at time  $t=0$ , i.e., still during the excitation pulse. Moreover, the shapes of the spectra show that the thermalization regime is also reached at surprisingly short times, typically within a few tens of picoseconds, as seen in Fig. 3. Originally, the authors interpreted these findings by suggesting a modification of the standard  $e-h$  interaction by complementing the conventional instantaneous  $e-h$  scatterings by acoustic-phonon-mediated multiple  $e-h$  scattering events.<sup>8</sup>

The present analysis maintains the standard description of  $e-h$  scattering, but attempts to explain the data by including the ionization of neutral donors and the corresponding recapture of free electrons as an additional electronic relaxation channel.

Section II begins with a description of the transport model underlying our  $k$ -space Monte Carlo simulations of the conventional carrier-phonon-acceptor dynamics. The failure of the simulations to reproduce the measured spectra will then motivate the additional consideration of the well-known partial compensation of Ge as a dopant in GaAs. In thermal equilibrium the donors are ionized; thus they had not previously been considered as inelastic scattering agents. How-

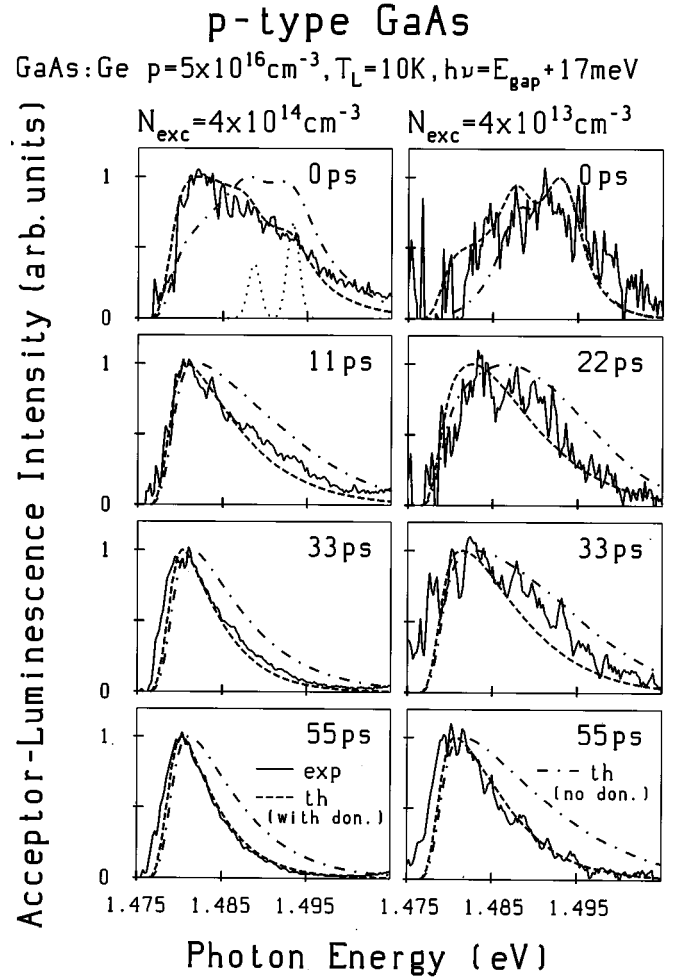


FIG. 2. Band-to-acceptor luminescence in  $p$ -doped GaAs ( $p=5 \times 10^{16} \text{ cm}^{-3}$ ); for  $N_{\text{exc}}=4 \times 10^{14} \text{ cm}^{-3}$  and for  $N_{\text{exc}}=4 \times 10^{13} \text{ cm}^{-3}$ ; solid lines: experiment (shown are the data of Ref. 8 without the originally included smoothing procedure); dashed-dotted lines: theory without Ge donors; dashed lines: theory including Ge donors; dotted lines: (calculated) electronic excitation spectrum with the two transition peaks from the hh and lh valence bands (Ref. 6).

ever, the finite experimental pulse-repetition rate together with the slow donor-acceptor recombination results in a substantial fraction of neutral donors, whose ionization by electrons opens a very fast and effective scattering channel for the initial broadening and the cooling of the photoexcited electron distribution. The remaining part of Sec. II presents the details of this improved scattering scenario and its confirmation by the good agreement between the measured and the simulated spectra, and provides further experimental evidence of the important role of donor scattering in our GaAs:Ge data. Section III contains a summary of our results.

## II. THEORY AND RESULTS

The Ensemble Monte Carlo (EMC) technique provides a very efficient way of solving time-dependent Boltzmann-type kinetic equations for hot carriers in semiconductors.<sup>15</sup> The experimental conditions restrict the present transport problem to a description of a spatially homogeneous system of photoexcited electrons and holes; at experimental lattice

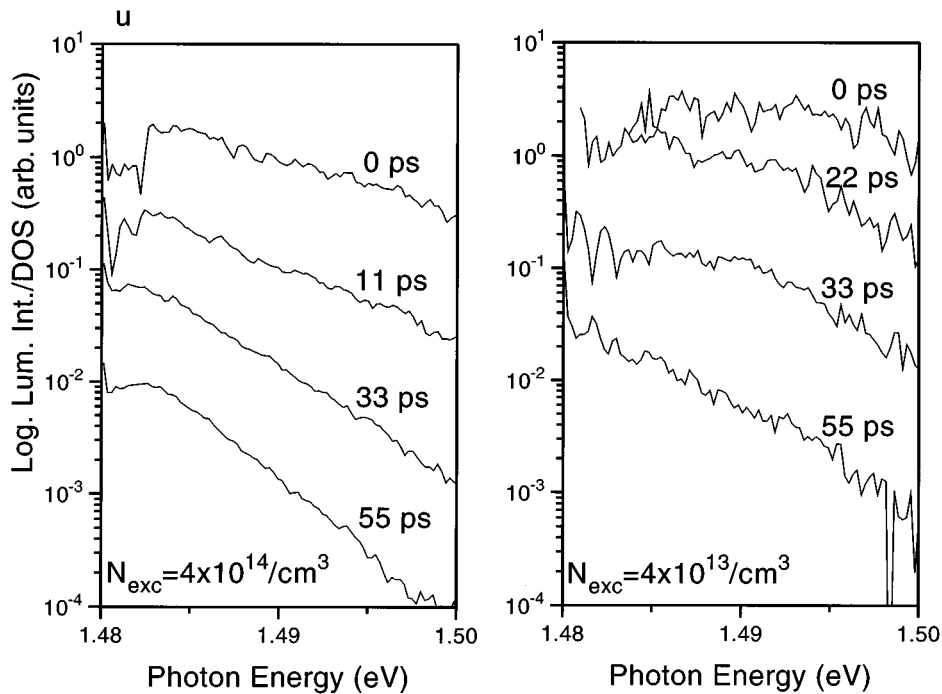


FIG. 3. Semilogarithmic plot of electron distribution functions, as obtained from the experimental spectra of Fig. 2.

temperatures of 10 K, practically all holes of the doping background are bound to their acceptors. As details of the band structure, such as the nonparabolicity and warping of the valence bands, should have a minor influence on the electronic relaxation rates,<sup>8</sup> all carriers were treated as quasifree with appropriate effective masses ( $m_e = 0.067m_0$ ,  $m_{lh} = 0.45m_0$ , and  $m_{hh} = 0.082m_0$ ).

The essential ingredients of our EMC, which have been detailed in a foregoing paper,<sup>3</sup> can be summarized as follows. As already mentioned, the EMC simulation is a method of solving the coupled time-dependent Boltzmann equations for electrons and holes. In our case these equations included the rates for the laser-pulse generation of electron-hole pairs and the additional ionization and capture rates of carriers at impurities. Typically our simulations contained 30 000–50 000 simulated particles. The simulation starts by introducing the photogenerated particles according to the temporal and spectral shapes of the excitation pulse. Using random numbers in combination with the quantum-mechanical probability distributions for the differential and total generation, capture and scattering cross sections, one follows the time evolution of the ensemble of particles in  $k$  space, obtaining the distribution functions of the carriers as functions of time during and after the excitation pulse. For our present case of band-acceptor luminescence, the simulated electron distribution function directly gives the luminescence spectrum, apart from a trivial density-of-states factor. However, an additional frequency convolution was necessary, as the acceptor levels are slightly broadened by their interaction with the ionized acceptors and donors always present in GaAs:Ge. Finally a convolution of this “intrinsic” luminescence spectrum with respect to time and frequency had to be performed to include the spectral and temporal details of the experimental detection procedure.<sup>8,9</sup>

In our simulation of the carrier-phonon-acceptor scenario, all standard types of carrier-carrier and the most effective carrier-phonon scatterings were taken into account. In addition

to the various carrier-carrier interactions, the non-phononic dynamics included the ionization of neutral acceptors [ $E_{ion}(\text{Ge}) = 40.5$  meV] by sufficiently energetic electrons and the corresponding recapture processes, as well as non-phononic  $lh \leftrightarrow hh$  inter-valence-band transitions induced by  $e-h$  and  $h-h$  scatterings.<sup>16</sup> As already discussed in Ref. 8, excitonic as well as exchange effects were assumed to be negligible under the present experimental conditions. The carrier-phonon dynamics contained the polar-optic coupling of electrons and holes to LO phonons, the optic deformation-potential coupling of holes to both LO and TO phonons, the corresponding phononic inter-valence-band transitions of heavy and light holes, and the deformation-potential coupling of electrons and holes to acoustic phonons. However, at the low excitation energies and lattice temperatures of our present concern, all types of phonons play a minor role: the optical phonons because of their low mode occupation and high energetic emission threshold, and the acoustic phonons because of their low scattering rates. As the energetic threshold for acceptor ionization is even higher than that for LO-phonon emission, this relaxation channel also turned out to be completely ineffective.

Due to our neglect of the donors, we had to simulate a situation where carrier-carrier scattering should prevail at early times (0–5 ps). Moreover, because of the pronounced mass differences between electrons and holes, electron-electron scattering would strongly dominate the initial broadening and internal thermalization of the electrons. Only at later times should electron-phonon and electron-hole scatterings initiate a noticeable energy dissipation of the electrons.

The free-carrier screening of all Coulombic interactions was treated by use of a quasidynamical version of the standard long-wavelength limit of the static random-phase approximation (RPA) dielectric function. This version had been successfully applied in simulations of highly excited and dense electron-hole plasmas in GaAs-type semiconductors.<sup>3,13</sup> Following this earlier work we checked

our screening model by comparing the results of the EMC calculation with a molecular-dynamics simulation of the electron-hole system. In this latter approach no carrier-phonon interactions are taken into account. However, as explained above, in our early-time spectra this dissipative interaction with phonons as well as the acceptor ionizations are negligible. For each simulated particle molecular dynamics replaces its instantaneous intercarrier scattering events of the kinetic  $k$ -space formulation by the continuous action in  $\vec{r}$  space of the total electric field created by all partner carriers of the ensemble. By following the trajectories of all particles, the velocity distributions and therefore the  $k$ -space distribution functions are found as functions of time. This is a purely classical approach, well suited for nondegenerate carrier systems like those of our present interest. Its main advantage over the Boltzmann description is the automatic inclusion of all higher-order  $N$ -particle correlations, improving over the screening problematics enforced by the use of instantaneous scattering events and of the Stosszahlansatz in the Boltzmann approach. A very good agreement between the results of the EMC and molecular dynamics gave further support to our treatment of the free-carrier screening.

The comparison between the EMC results for the standard carrier-phonon-acceptor system (dashed-dotted lines) and the experimental spectra (full lines) is shown in Fig. 2. We note pronounced discrepancies. At longer times (11–55 ps) the calculated high-energy parts of the spectra are systematically too high, and the corresponding asymptotic slopes lead to electron temperatures roughly 20° higher than the experimental ones. Both these findings indicate that a very effective energy-loss mechanism was missing in our scattering scenario. At short times the experimental data show a stronger broadening, and in particular a much faster population of the low-energy band states, again indicating the presence of an additional energy-dissipation mechanism.

As the most promising candidate for such a fast and efficient energy-relaxation channel, we next included the interaction of free carriers with neutral Ge donors. The presence of a relatively large number of neutral donors is the consequence of the fact that substitutional Ge in GaAs can act as an acceptor and as a donor, with a respective concentration ratio of roughly 3:1.<sup>8</sup> It is experimentally well documented by a long-lived donor-acceptor luminescence. In our experiments, the donor-acceptor recombination rate, which in equilibrium would lead to full compensation, was smaller than the repetition rate of the laser-excitation pulses, leading to a partial neutralization of donors. Adding capture of electrons at donors and donor ionization to our transport model, we included the 1s ground state and the first (2s) excited state as representative donor levels, as schematically shown in Fig. 4. The corresponding thermal-equilibrium bound- and free-state occupations as functions of temperature<sup>17</sup> are plotted in Fig. 5. Figure 6 shows the underlying scattering rates at 0 and 10 ps, as calculated using simple hydrogenic  $s$ -state wave functions.<sup>18</sup> Our best results were obtained by assuming the quasistationary concentration of neutral Ge donors to be eight and 15 times the calculated excitation density in our higher- and lower-density experiment, respectively. This choice of the proportionality factors was further supported by total-luminescence data, as will be shown below.

Ge donors have a much higher cooling efficiency than Ge

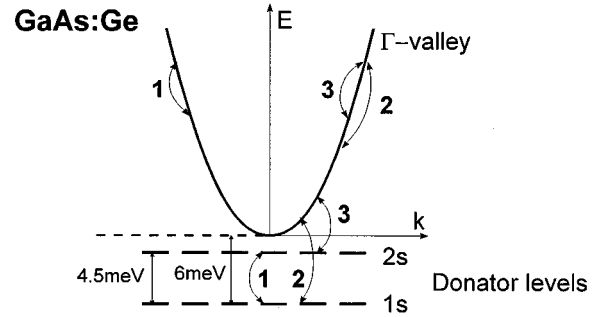


FIG. 4. Schematic representation of the two-level model for the electron-donor dynamics.

acceptors and LO phonons because of the small ionization energy of the Ge donors (6 meV as compared to the acceptor-ionization energy of 40.5 meV and the LO-phonon energy of 36.4 meV) and the correspondingly smaller energetic threshold for an inelastic scattering event. As a consequence, the interplay of electron captures at donors and of collision-induced ionizations of donors turned out to lead to net donor-ionization rates high enough to provide a fast and efficient energy-loss channel for the photoexcited electrons. The resulting improvement of the calculated mean electron

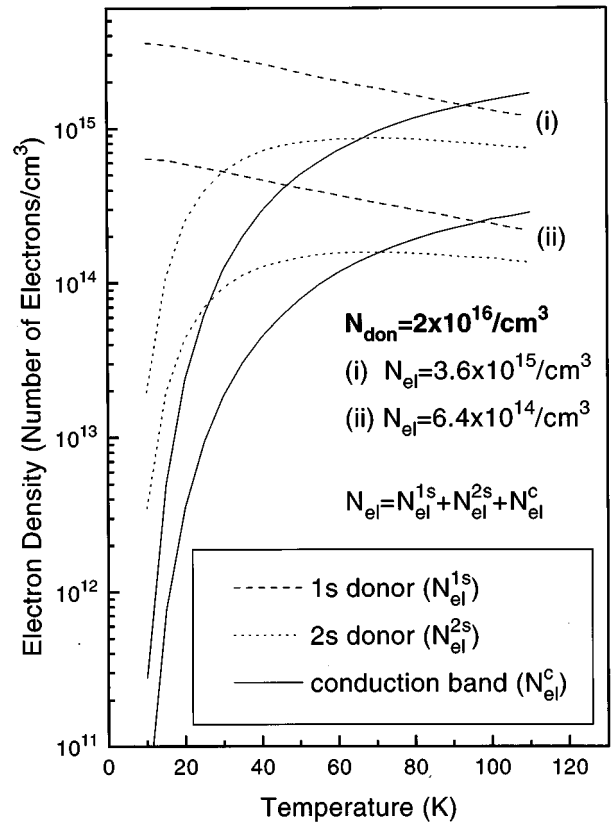


FIG. 5. Thermal-equilibrium mean free and bound-state occupations as functions of temperature;  $N_{\text{don}}$ : total number of donor states.  $N_{\text{el}}$ : total number of electrons. (i)  $N_{\text{el}} = 3.6 \times 10^{15} \text{ cm}^{-3}$ , and (ii)  $N_{\text{el}} = 6.4 \times 10^{14} \text{ cm}^{-3}$ , corresponding to (i)  $N_{\text{exc}} = 4 \times 10^{14} \text{ cm}^{-3}$ , and (ii)  $N_{\text{exc}} = 4 \times 10^{13} \text{ cm}^{-3}$ .

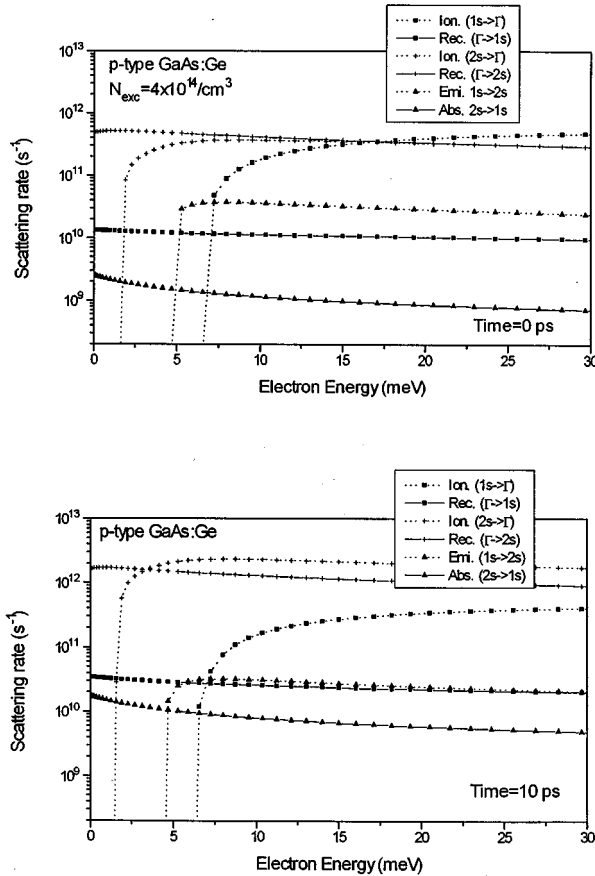


FIG. 6. Scattering rates for the electron-donor scattering model of Fig. 4; upper part:  $t=0$  ps; lower part:  $t=10$  ps.

energies is obvious from a comparison of the solid lines in Fig. 7 with the experimental points (obtained from the slopes in Fig. 3) and with the much too slow cooling found by neglecting the donors (dotted lines). Figure 7 also shows the mean energies obtained by taking only the donor  $1s$  ground state into account (dashed lines). This simplest possible donor model results in a too fast initial cooling followed by a practically dissipationless regime due to a very effective recombination heating.<sup>19,20</sup> Both these unfavorable effects are strongly reduced by the inclusion of the  $2s$  excited donor state. Here the  $2s \leftrightarrow \Gamma$  processes have the highest rates. While the  $1s \leftrightarrow \Gamma$  dynamics remains practically unchanged, the  $2s$  states are soon being filled up, partially compensating for the fast initial cooling and leading to a very good agreement with the experimental data. This  $2s$ -state filling could have also been inferred from Fig. 5 by invoking the conventional carrier-temperature concept: any laser-induced electron heating should strongly increase the  $2s$ -state occupation over its low initial value at 10 K.

In Fig. 2 we finally compare the calculated band-acceptor-luminescence spectra, obtained by inclusion of donors, with the experimental ones, finding a very good agreement between theory (dashed lines) and experiment (full lines). Here it should be noted that, especially in the high-density case, the experimental onset of the spectra is generally shifted a few meV below the nominal band gap. This energy shift can be explained by the the plasma-induced band-gap renormal-

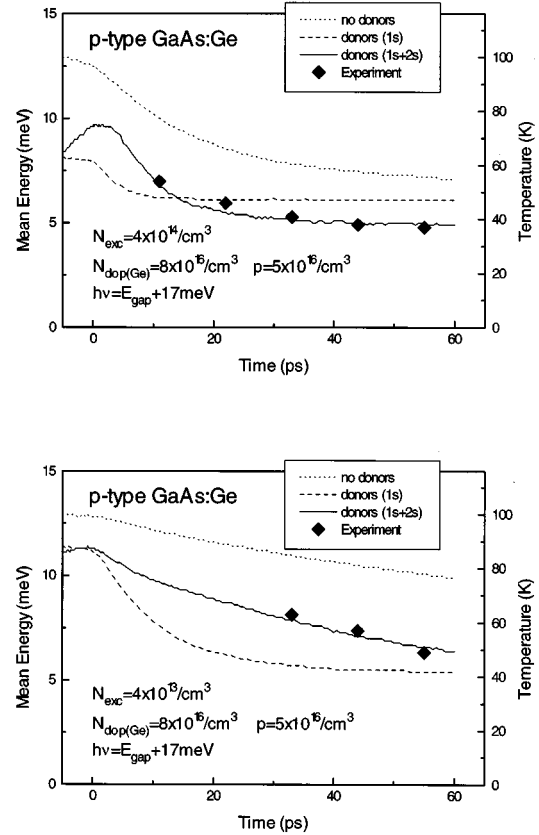


FIG. 7. EMC-simulated mean electron energies; full lines: including Ge donors; dotted lines: without Ge donors; upper part: for  $N_{\text{exc}}=4 \times 10^{14} \text{ cm}^{-3}$ ; lower part: for  $N_{\text{exc}}=4 \times 10^{13} \text{ cm}^{-3}$ ; squares: experimental values from well-established Maxwellian time regime.

ization. It can be estimated<sup>21</sup> to amount, depending on the carrier temperature, to 1–3 meV for the higher densities and to 1 meV for the low-excitation case, in agreement with the onset of the experimental spectra.

A comparison of the calculated and experimentally determined carrier temperatures, as obtained from the near-exponential slopes of the spectra, again shows good agreement. As a minor technical point we mention that the logarithmic representations of the experimental data in Fig. 3 contain the already mentioned foldings, and therefore do not directly yield the temperature as the slope of the spectra.

The only free parameter used in our final theoretical model was the number of neutral donors before each laser pulse excites the electron-hole pairs. Our experimental verification of a near-linear relation between the intensity of the donor-acceptor pair recombination and the excitation density justifies our assumption that the number of neutral donors scales with the excitation density. Let us, then, check on our choice of the absolute numbers, i.e., the ratios 8 for the higher and 15 for the lower excitation densities. This can be done by subtracting, as in all previous luminescence data, the stationary  $1s$ -donor-acceptor background and comparing the time behavior of the intensity of all remaining electron-acceptor recombinations with the number of free and  $2s$  electrons as calculated under the assumption of approximately equal  $\Gamma$ -acceptor and  $2s$ -acceptor transition rates.

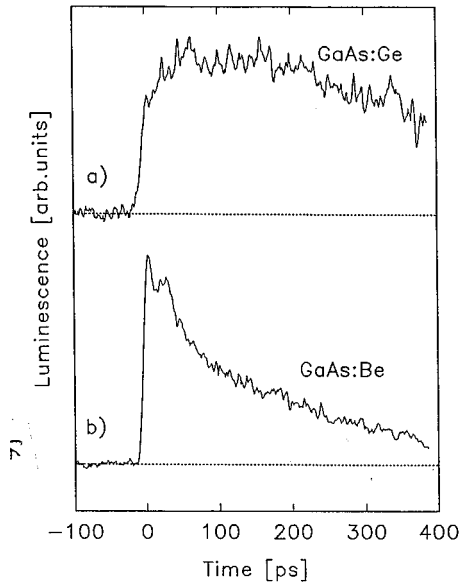


FIG. 8. Time evolution of the total (i.e., frequency-integrated) experimental band-acceptor luminescence for *p*-type GaAs:Ge and GaAs:Be.

Figure 8 compares the total (i.e., frequency-integrated) luminescence for GaAs:Ge and for a conventionally doped material, i.e., GaAs:Be, as functions of time.<sup>22</sup> In contrast to the eventual decrease of the luminescence after typically a few ps in GaAs:Be, the total acceptor luminescence in GaAs:Ge increases in time due to the ionization and  $1s$ - $2s$  excitation of neutral donors, as reflected in the calculated number of free and  $2s$  electrons. This correspondence is shown in the upper part of Fig. 9, and the separate densities of free and  $2s$  electrons in the lower part. The close agreement between the time evolution of the luminescence and that of the various calculated electron densities substantiates the specific choice of the proportionalities between the absolute neutral-donor densities and the excitation densities in our calculations.

Moreover, GaAs:Be as a reference material provides an additional, and direct, evidence for the decisive scattering contributions of donors to our GaAs:Ge spectra: the initial electron distribution function in GaAs:Be is significantly more structured due to the absence of the additional donor scatterings, as has been discussed in Ref. 23 and can be seen from a comparison of our Fig. 2 with Fig. 1 of Ref. 23.

### III. SUMMARY

The recent experimental finding of an unexpectedly fast broadening, thermalization, and cooling of a narrow photoexcited electron distribution in the time-resolved band-to-acceptor luminescence of GaAs at very low excitation den-

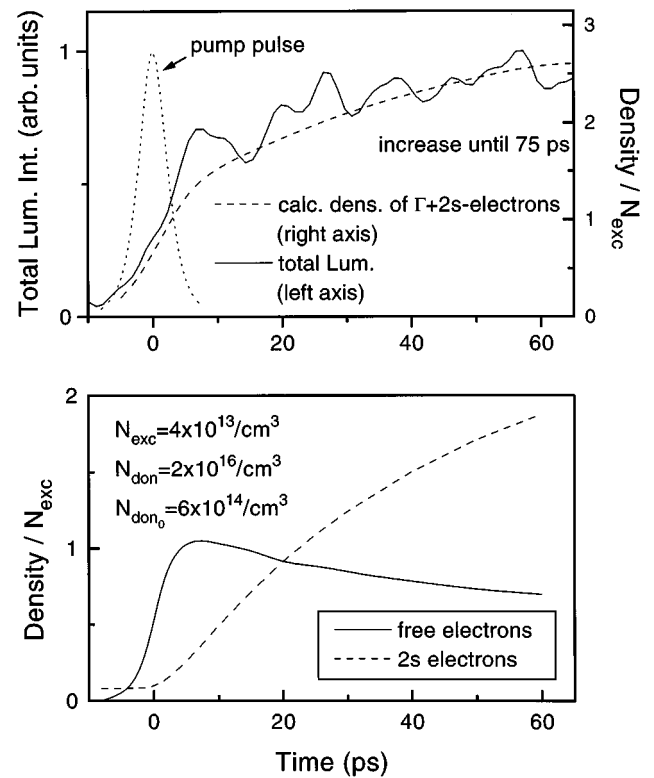


FIG. 9. Upper part: spectrally integrated experimental acceptor luminescence (full line) and density of ( $\Gamma+2s$ ) electrons (dotted line) as functions of time; lower part: calculated free-electron density (full line) and  $2s$ -state occupation (dashed line) as functions of time.

sities has been theoretically analyzed by state-of-the-art  $k$ -space ensemble Monte Carlo and  $\vec{r}$ -space molecular-dynamics simulations.

Considering the coupled system of electrons, holes, and acceptors, extensive ensemble Monte Carlo calculations and complementary molecular-dynamics simulations could not explain the measured broadenings. However, good agreement was found after taking account of the relatively frequent ionizations of neutral Ge donors by free carriers. It turned out that this additional scattering mechanism provides a very efficient energy-relaxation channel for the photoexcited electrons, accelerating both their initial distribution broadening and their ensuing thermalization.

In addition to the analysis of the thermalization regime, the later cooling stage of the electronic evolution has been studied by a comparison of the increase of the near-exponential slope of the measured and the calculated band-acceptor luminescence spectra. Here the inclusion of Ge donors was also necessary to find agreement between theory and experiment.

\*Dept. of Physics and Astronomy, University of Pittsburgh, Pittsburgh, PA 15260.

<sup>1</sup>J. Shah, *Solid-State Electron.* **32**, 1051 (1989).

<sup>2</sup>T. Elsässer, J. Shah, L. Rota, and P. Lugli, *Semicond. Sci. Technol.* **7**, B144 (1992); *Phys. Rev. Lett.* **66**, 1757 (1991).

<sup>3</sup>U. Hohenester, P. Supancic, P. Kocevar, X. Q. Zhou, W. Kütt, and

H. Kurz, *Phys. Rev. B* **47**, 13 233 (1992).

<sup>4</sup>D. N. Mirlin, I. Ya. Karlik, L. P. Nikitin, I. I. Reshina, and V. F. Sapega, *Solid State Commun.* **37**, 757 (1980).

<sup>5</sup>R. G. Ulbrich, J. A. Kash, and J. C. Tsang, *Phys. Rev. Lett.* **62**, 949 (1989).

<sup>6</sup>G. Fasol, W. Hackenberg, H. P. Hughes, K. Ploog, E. Bauser, and

- H. Kano, Phys. Rev. B **31**, 1461 (1990).
- <sup>7</sup>Y. Sun and C. Stanton, Phys. Rev. B **43**, 2285 (1991).
- <sup>8</sup>D. W. Snoke, W. W. Rühle, Y.-C. Lu, and E. Bauser, Phys. Rev. B **45**, 10 979 (1992).
- <sup>9</sup>D. W. Snoke, W. W. Rühle, Y.-C. Lu, and E. Bauser, Phys. Rev. Lett. **68**, 990 (1992).
- <sup>10</sup>L. Rota and D. K. Ferry, Semicond. Sci. Technol. **9**, 469 (1994).
- <sup>11</sup>J. H. Collet, Phys. Rev. B **39**, 7659 (1989).
- <sup>12</sup>J. H. Collet, W. W. Rühle, M. Pugnet, K. Leo, and A. Million, Phys. Rev. B **40**, 12 296 (1989).
- <sup>13</sup>U. Hohenester, P. Supancic, P. Kocevar, and L. Rota, in Proceedings of the 8th Vilnius Symposium on Ultrafast Phenomena in Semiconductors [Lithuania J. Phys. **32**, 117 (1992)].
- <sup>14</sup>P. Kocevar, Phys. Scr. **T45**, 210 (1992).
- <sup>15</sup>C. Jacoboni and P. Lugli, *The Monte Carlo Method for Semiconductor Device Simulation* (Springer Verlag, Wien, 1989).
- <sup>16</sup>J. F. Young, P. Kelly, and N. L. Henry, Phys. Rev. B **36**, 4535 (1987).
- <sup>17</sup>J. S. Blakemore, *Semiconductor Statistics* (Pergamon, New York, 1962).
- <sup>18</sup>L. I. Schiff, *Quantum Mechanics*, 2nd ed. (MacGraw-Hill, New York, 1955).
- <sup>19</sup>D. Bimberg and J. Mycielski, J. Phys. C **19**, 2363 (1986).
- <sup>20</sup>K. Leo and W. W. Rühle, Solid State Commun. **62**, 659 (1987).
- <sup>21</sup>R. Zimmermann, Phys. Status Solidi B **146**, 371 (1988).
- <sup>22</sup>R. M. Hannak, Ph.D. thesis, Leopold-Franzens-Universität Innsbruck, Austria, 1995.
- <sup>23</sup>R. M. Hannak and W. W. Rühle, Phys. Rev. B **50**, 15 445 (1994).